



# PM<sub>2.5</sub> water-soluble elements in the southeastern United States: automated analytical method development, spatiotemporal distributions, source apportionment, and implications for health studies

T. Fang<sup>1</sup>, H. Guo<sup>1</sup>, V. Verma<sup>1,a</sup>, R. E. Peltier<sup>2</sup>, and R. J. Weber<sup>1</sup>

<sup>1</sup>School of Earth and Atmospheric Sciences, Georgia Institute of Technology, Atlanta, GA, USA

<sup>2</sup>School of Public Health and Health Sciences, University of Massachusetts, Amherst, MA, USA

<sup>a</sup>now at: Department of Civil and Environmental Engineering, University of Illinois Urbana-Champaign, Champaign, IL, USA

Correspondence to: R. J. Weber (rodney.weber@eas.gatech.edu)

Received: 15 May 2015 – Published in Atmos. Chem. Phys. Discuss.: 24 June 2015

Revised: 5 October 2015 – Accepted: 6 October 2015 – Published: 21 October 2015

**Abstract.** Water-soluble redox-active metals are potentially toxic due to its ability to catalytically generate reactive oxygen species (ROS) in vivo, leading to oxidative stress. As part of the Southeastern Center for Air Pollution and Epidemiology (SCAPE), we developed a method to quantify water-soluble elements, including redox-active metals, from a large number of filter samples ( $N = 530$ ) in support of the center's health studies. PM<sub>2.5</sub> samples were collected during 2012–2013 at various sites (three urban, two rural, a near-road site, and a road-side site) in the southeastern United States, using high-volume samplers. Water-soluble elements (S, K, Ca, Ti, Mn, Fe, Cu, Zn, As, Se, Br, Sr, Ba, and Pb) were determined by extracting filters in deionized water and re-aerosolized for analyses by X-ray fluorescence (XRF) using an online aerosol element analyzer (Xact, Cooper Environmental). Concentrations ranged from detection limits (nominally 0.1 to 30 ng m<sup>-3</sup>) to 1.2 μg m<sup>-3</sup>, with S as the most abundant element, followed by Ca, K, Fe, Cu, Zn, and Ba. Positive matrix factorization (PMF) identified four factors that were associated with specific sources based on relative loadings of various tracers. These include brake/tire wear (with tracers Ba and Cu), biomass burning (K), secondary formation (S, Se, and WSOC), and mineral dust (Ca). Of the four potentially toxic and relatively abundant metals (redox-active Cu, Mn, Fe, and redox-inactive Zn), 51 % of Cu, 32 % of Fe, 17 % of Mn, and 45 % of Zn were associated with the brake/tire factor. Mn was mostly associated with the mineral dust factor (45 %). Zn was found in a mixture of fac-

tors, with 26 % associated with mineral dust, 14 % biomass burning, and 13 % secondary formation. Roughly 50 % of Fe and 40 % of Cu were apportioned to the secondary formation factor, likely through increases in the soluble fraction of these elements by sulfur-driven aerosol water and acidity. Linkages between sulfate and water-soluble Fe and Cu may account for some of the past observed associations between sulfate/sulfur oxide and health outcomes. For Cu, Mn, Fe, and Zn, only Fe was correlated with PM<sub>2.5</sub> mass ( $r = 0.73$ – $0.80$ ). Overall, mobile source emissions generated through mechanical processes (re-entrained road dust, tire and brake wear) and processing by secondary sulfate were major contributors to water-soluble metals known to be capable of generating ROS.

## 1 Introduction

Many fine particle (PM<sub>2.5</sub>) chemical components have been reported as potential contributors to particle toxicity that can lead to various adverse health endpoints, including secondary sulfates (Atkinson et al., 2010; Maynard et al., 2007; Pope et al., 2002), elemental carbon (Kleinman et al., 2007; Brunekreef et al., 1997), metals (Gasser et al., 2009; Burchiel et al., 2005; Pope et al., 2002; Burnett et al., 2000), organic carbon (Kleinman et al., 2007; Nel et al., 2001), semi-volatile organic species (Seagrave et al., 2005; Seagrave et al., 2002),

and polycyclic aromatic hydrocarbons (PAHs) (Lundstedt et al., 2007; Burchiel et al., 2005). Identifying the components of aerosols that are responsible for health effects provides a means for effective air quality mitigation by controlling specific sources.

Metals are known to exert pro-oxidant and pro-inflammatory effects in the respiratory system (Cho et al., 2011; Li et al., 2010), and the water-soluble fraction of metals are of special interest as they are more bioavailable (Heal et al., 2005; Shi et al., 2003) and may have a higher risk potential. For example, a study with concentrated ambient particles (CAPS) associated inflammatory endpoints (pulmonary and hematological responses) to water-soluble Fe/Se/S and Cu/Zn/V factors (Huang et al., 2003). Another CAPS study found that the plasma fibrinogen levels (a coronary risk indicator) in spontaneously hypertensive rats were better correlated with water-soluble metals (especially Zn) than total PM mass (Kodavanti et al., 2005). PM<sub>2.5</sub> water-soluble metals were found to be significantly associated with small reductions in birth weight (Darrow et al., 2011) and daily pre-term birth rates (Darrow et al., 2009) in an Atlanta, GA, study.

Water-soluble transition metal toxicity may be due to their ability to generate free radicals, for example, via redox cycling with biological reductants (Chevion, 1988; Stohs and Bagchi, 1995). Transition metals have varying oxidation states, thus metals, especially Fe and Cu, can act as a catalyst for the reactions, e.g., Fenton reaction that convert hydrogen peroxide to the more toxic hydroxyl radicals (Licochev and Fridovich, 2002; Stohs and Bagchi, 1995). Metal-mediated formation of free radicals may lead to DNA modifications, enhanced lipid peroxidation, and altered calcium and sulfhydryl homeostasis (Valko et al., 2005). Water-soluble transition metals have been identified as the potential contributors to reactive oxygen species (ROS) production by different ROS probes such as the DTT (dithiothreitol) (Charrier and Anastasio, 2012), AA (ascorbate acid) (Strak et al., 2012; Fang et al., 2015b), and macrophage (Saffari et al., 2014; Verma et al., 2010) assays.

Since most metals in PM have low solubilities (e.g., Zn ~ 50 %, Cu and Mn 10–40 %, Fe < 10 %) (Birmili et al., 2006; Espinosa et al., 2002), total element concentrations may not represent the potential effects of the roles of redox-active metals on human health. The objective of this work, within the framework of the Southeastern Center for Air Pollution & Epidemiology (SCAPE) study, was to provide a reliable measurement of PM<sub>2.5</sub> water-soluble element concentrations from filter samples collected at seven sites in the southeastern USA that represent different degrees of anthropogenic and traffic influence. A cost-effective and automated method was required since over 500 filters were available for analyses. The resulting unique large and comprehensive data set allowed for robust statistical analyses and has informed studies on particle ROS generating activities based on the DTT (Verma et al., 2015; Verma et al., 2014) and AA assays (Fang et al., 2015b). The data have provided new

insights into the health effects of particulate water-soluble metals. This work focuses on a description of the measurement techniques, discussion on the spatiotemporal distribution, and source apportionment of water-soluble elements, with a specific focus on four important health-related water-soluble metals (Fe, Cu, Mn, and Zn).

## 2 Methods

The present work involves measuring water-soluble elements from filter extracts by re-aerosolizing the extract and sampling with an online X-ray fluorescence (XRF) instrument. The ambient mass concentrations of the following water-soluble elements were quantified: S (sulfur), Ca (calcium), K (potassium), Fe (iron), Cu (copper), Zn (zinc), Ba (barium), Pb (lead), As (arsenic), Sr (strontium), Se (selenium), Br (bromine), Mn (manganese), and Ti (titanium). S is also included in the discussion since it is a source indicator for secondary processing.

### 2.1 Sampling sites and filter preparation

#### 2.1.1 Sampling sites

As part of the SCAPE study, 23 h integrated PM<sub>2.5</sub> samples were collected on pre-baked (max temperature: 550 °C, time ramp: 3.5 h) quartz filters (Pallflex<sup>®</sup> Tissuquartz<sup>™</sup>, 8 × 10 inches) from noon to 11 a.m. the following day with high-volume (Hi-Vol) samplers (Thermo Anderson, flow rate normally 1.13 m<sup>3</sup> min<sup>-1</sup>) in Atlanta, GA, Birmingham and Centerville, AL, and East St. Louis, IL. The sites were

1. Jefferson Street, GA (JST), a central site representative of the Atlanta urban environment, also a stationary site in this study where one Hi-Vol sampler was operated for most of the study period;
2. Yorkville, GA (YRK), a rural environment, situated in an agricultural region located approximately 70 km west of JST;
3. Road side, GA (RS), adjacent to an interstate highway (I75/85) in midtown Atlanta;
4. Georgia Tech, GA (GT), a rooftop site on Georgia Tech campus, roughly 30 m above ground level, 840 m from the RS site, providing an intermediate location between RS and the central urban site (JST);
5. Birmingham, AL (BHM), an urban site within a few kilometers of significant transportation and industrial sources;
6. Centerville, AL (CTR), the rural pair of BHM, surrounded by forests and a lightly traveled rural road;

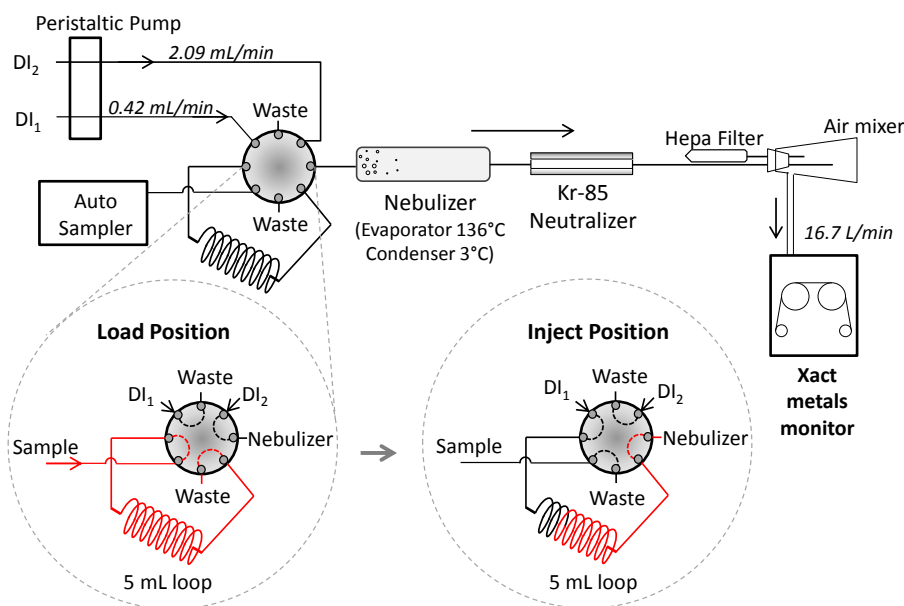


**Figure 1.** Schematic of automated system developed to measure elements in the water-soluble aerosol extracts using an online XRF element analyzer (Xact™ 625).

7. East St. Louis, IL (Sauvain et al., 2008), an urban residential/light commercial area approximately 3 km east of the central business district of St. Louis, MO.

JST, YRK, BHM, and CTR are all part of the Southeastern Aerosol Research and Characterization Study (SEARCH) network sites (Hansen et al., 2003). The sampling approach involved paired simultaneous measurements: one high-volume sampler always at JST and the other sampler moved among RS, GT and YRK on a monthly basis, during different seasons. Paired sampling at BHM and CTR was also undertaken for a month and coincided with the Southern Oxidant and Aerosol Study (SOAS). Detailed sampling schedule and map can be found in the Supplement (Table S1 and Fig. S1 in the Supplement). Samples were collected from June 2012 to September 2013. In November 2012, two Hi-Vol samplers were co-located at JST for side-by-side comparisons. A total of 530 filters were collected as part of the study. In all cases, collected filter samples were immediately wrapped in pre-baked aluminum foil and stored at  $-18^{\circ}\text{C}$  until analyzed.

### 2.1.2 Filter preparation

Four punches of the Hi-Vol filter ( $5.07\text{ cm}^2$  each) were extracted in 15 mL of deionized (DI) water ( $> 18\text{ M}\Omega\text{ cm}^{-1}$ ) in a sterile polypropylene centrifuge tube (VWR International LLC, Suwanee, GA, USA) by sonication (Ultrasonic Cleanser, VWR International LLC, West Chester, PA, USA) for half an hour. Extracts were then filtered using PTFE  $0.45\text{ }\mu\text{m}$  syringe filters (Fisherbrand™) to remove insoluble material; 120  $\mu\text{L}$  of high purity  $\text{HNO}_3$  (OmniTrace® Ultra

Nitric Acid, 67–70 %, EMD Millipore Corporation, Billerica, MA, USA) was then added to 6 mL of the extract (resulting  $\text{pH} \approx 0.7$ ) to ensure the suspension of all dissolved metals, and were then transferred to a 5 mL DIONEX autosampler vial (PolyVial™, Thermo Scientific). Some insoluble elements that are smaller than  $0.45\text{ }\mu\text{m}$  in diameter can be included in the water-soluble fractions defined by this method. It is also noted that water-soluble element concentrations are operationally defined by the extraction method, and may differ from how elements are dissolved in vivo.

### 2.2 Methods for measuring water-soluble element concentration

A Xact™ 625 automated multi-metals monitor (Cooper Environmental, OR, USA) was used to measure the concentration of elements in the liquid samples. The Xact collects particles on a reel-to-reel (RTR) Teflon filter tape, sampling at  $16.7\text{ L min}^{-1}$  for a user selected time interval (30 min in this case), resulting in a concentrated PM spot on the tape. After the preset sampling interval, the tape is automatically advanced, positioning the PM spot for non-destructive XRF analyses to quantify the mass of multiple elements. At the same time, the next sampling is initiated on a fresh tape spot. XRF response is calibrated using a series of metal film standards on B36 mount nucleopore membranes (Nano XRF, Fort Worth, TX, USA), including appropriate interference element analytes. With each sample, the Xact also includes a measurement of pure palladium as an internal standard to automatically adjust the detector energy gain.

To introduce water-soluble metals from filter extracts in Xact, a computer-controlled auto-sampling system was set up using a Dionex autosampler, a multi-port injection valve and a continuous flow nebulizer so that sampling and analysis could be performed continuously, except during daily automated quality assurance checks (~ 1 h). A schematic diagram of the overall system is shown in Fig. 1. At “load” position, liquid sample (at least 6 mL) was loaded by a DIONEX automated sampler (AS40, DIONEX Corporation, Sunnyvale, CA, USA) through a SelectPro two-position fluid processor valve (Alltech, Deerfield, IL, USA) to a 5 mL PEEK sample loop (Upchurch Scientific, Inc., Oak Harbor, WA). After 2.5 min, at which point the sample loop had been completely filled with extract liquid from the Dionex autosampler, the valve was switched to the “inject” position and all 5 mL of sample injected to an ultrasonic nebulizer (CETAC U5000 AT+, CETAC Technologies, Omaha, NE, USA) via a carrier DI flow of 0.42 mL min<sup>-1</sup> (DI<sub>1</sub>, Fig. 1) propelled by a peristaltic pump (Ismatec, Cole-Parmer Instrument Company, Vernon Hills, IL, USA). In the continuous flow ultrasonic nebulizer, liquid sample was converted to a fine aerosol spray and directed by filtered carrier room air of 1.62 L min<sup>-1</sup> through an evaporator at 136 °C followed by a condenser at 3 °C. The dry aerosolized sample was neutralized by a Kr-85 (Model 3077A, TSI) ion source and then mixed with clean filtered (Pall HEPA Capsule) make-up air drawn into the Xact and through the filter tape by the Xact’s flow control system. After 14 min, at which point all sample in the sample loop had been transferred to the Xact filter tape, the system switched to load position again, and DI water with HNO<sub>3</sub> (final concentration = 2 %) was loaded onto the sample loop (2.5 min), after which the system switched to inject position again, and the 2 % HNO<sub>3</sub> was directed to the nebulizer and the Xact. This cycle was performed to wash off any metal residuals in the liquid system. After 11 min, the filter tape was automatically advanced to a position where total mass for each element from the sample was measured by XRF analysis. At the same time, the system repeated the process for measuring the next sample (i.e., load sample-inject sample-load 2 % HNO<sub>3</sub>-inject 2 % HNO<sub>3</sub>, 2.5-14-2.5-11 min cycle). To further ensure no carry-over between samples, a faster DI flow (DI<sub>2</sub>, 2.09 mL min<sup>-1</sup>, Fig. 1) was used for flushing while the SelectPro valve was at the load position. Inserting 2 % HNO<sub>3</sub> between samples was found to be an effective method to eliminate carry-over between samples (Fig. S2, Supplement).

The final ambient concentration of each element was calculated as follows:

$$C_a = \frac{(C_{\text{sample}} V_{\text{sample}} - C_{\text{blank}} V_{\text{blank}})}{m} \times \frac{15 \text{ mL} \frac{A_{\text{filter}}}{A_{\text{punches}}}}{5 \text{ mL} \times Q t}, \quad (1)$$

where  $C_a$  is the specific element ambient concentration (ng m<sup>-3</sup>);  $C_{\text{sample}}$  ( $C_{\text{blank}}$ ) and  $V_{\text{sample}}$  ( $V_{\text{blank}}$ ) are the concentration of element (ng m<sup>-3</sup>) and volume of air (m<sup>3</sup>) drawn

through the filter tape for sample (blank), respectively, both reported by the XRF in the 30 min sampling time. the volume of DI water used for the filter extraction is 15 mL and the sample liquid volume loaded to the Xact is 5 mL.  $A_{\text{filter}}$  is the total particle collection area of the Hi-Vol filter (m<sup>2</sup>) and  $A_{\text{punches}}$  is the area used for this analysis (m<sup>2</sup>).  $Q$  is the Hi-Vol sampling flow rate (~ 1.13 m<sup>3</sup> min<sup>-1</sup>) and  $t$  is the sampling duration (min).  $m$  is the calibration factor determined by multiple external element standard solutions, discussed below (Sect. 2.3).

A similar automated system with the DIONEX sampler, SelectPro valve, and a peristaltic pump was also used to measure water-soluble organic carbon (WSOC) on the extracts from the same Hi-vol filters. Filter extracts (~ 6 mL) that had been loaded into a 5 mL sample loop, were first passed through a 1 m Liquid Wave-guide Capillary Cell (LWCC-M-100; World Precision Instruments, Inc., FL, USA), where absorbance at 365 nm wavelength (BrC) was measured (not included in this work). The extracts then entered a TOC analyzer (Sievers Model 900, GE Analytical Instruments, Boulder, CO, USA) for determining WSOC concentration (Sullivan et al., 2006).

### 2.3 Calibration

Multiple element-ion standard stock solutions [(NH<sub>4</sub>)<sub>2</sub>SO<sub>4</sub>, CaCl<sub>2</sub>, (NH<sub>4</sub>)<sub>2</sub>Fe(SO<sub>4</sub>)<sub>2</sub>, CuSO<sub>4</sub>, ZnCl<sub>2</sub>, and MnCl<sub>2</sub>] were prepared by dissolving powders in DI water with HNO<sub>3</sub> (2 % final concentration) and stored in a refrigerator ( $T = 4$  °C). CuSO<sub>4</sub> and (NH<sub>4</sub>)<sub>2</sub>Fe(SO<sub>4</sub>)<sub>2</sub> were obtained from Sigma-Aldrich; CaCl<sub>2</sub>, MnCl<sub>2</sub>, and ZnCl<sub>2</sub> were obtained from Alfa Aesar; (NH<sub>4</sub>)<sub>2</sub>SO<sub>4</sub> was from Fisher Scientific. Final standard solutions were diluted from stock (20–200 times dilution), 2 % HNO<sub>3</sub> added, transferred to DIONEX vials, and ran through the same system as described above.

Figure 2 shows the system calibration using serial dilutions of multiple element-ion standards. Linear regression yielded  $r^2$  larger than 0.98 for all cases and similar slopes (0.47–0.60), indicating that the nebulizer efficiency and other losses in the system were not dependent on the specific element. Slopes from measured mass versus calculated mass of element-ion standard solutions for all standards were averaged and used as the calibration factor ( $m = 0.53 \pm 0.05$  in Eq. 1) to interpret all elements in samples. The intercepts were not included in the final ambient concentration calculation (Eq. 1) since the intercept of sample and blank cancel out after blank subtraction. The standards were made in the range of typical sample concentrations and the intercepts were negligible (< 2 % of typical ambient levels). One standard ion solution was measured for every five filter samples and the coefficients of variation (CV, calculated as standard deviation ( $\sigma$ )/mean, %) were less than 10 % throughout the analyses of all filters, indicating that the system was capable of stable and reproducible operation.

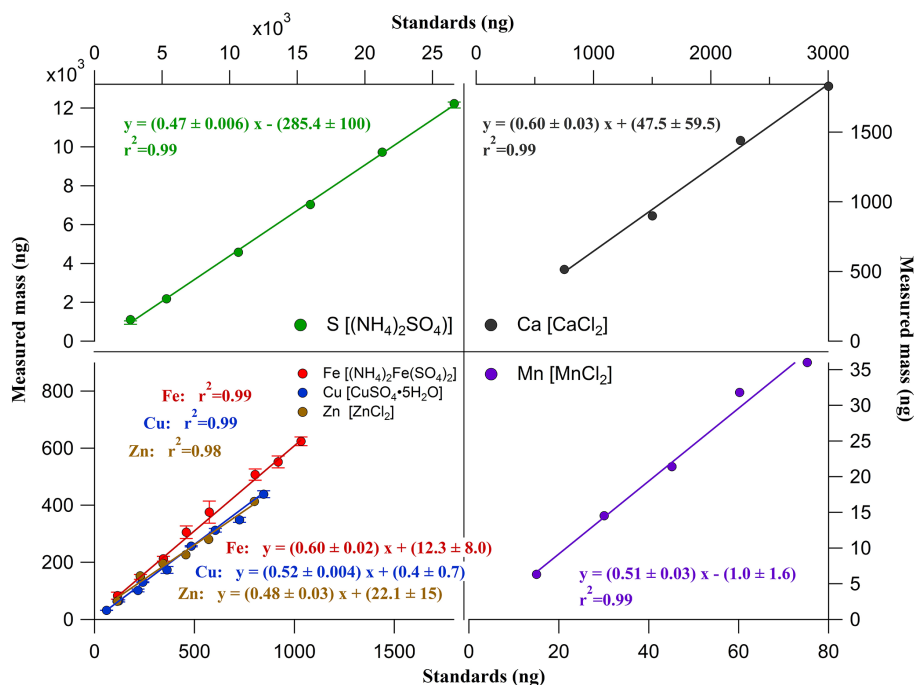


**Figure 2.** System calibration based on multiple element-ion standard solutions. Error bars represent the standard deviation of three replicates. Slopes and intercepts are based on orthogonal regression with errors as 1 standard deviation.

**Table 1.** Limits of detection (LOD), blanks ( $N > 40$ ) and uncertainties for all water-soluble elements.

Element	LOD, $\text{ng m}^{-3}$	Blank, $\text{ng m}^{-3}$	Analytical uncertainty, %	Sum of square of various uncertainties, %	Uncertainty from collocated measurements, %	Overall uncertainty, %
Sulfur (S)	6.19	6.64	2.19	7.77	2.38	8.13
Potassium (K)	16.45	11.80	2.47	9.89	6.06	11.63
Calcium (Ca)	29.64	32.23	2.38	10.46	11.76	15.87
Titanium (Ti)	0.09	0.06	15.79	21.08	18.68	28.22
Manganese (Mn)	0.11	0.06	3.57	8.54	6.49	10.74
Iron (Fe)	3.11	1.54	12.59	13.94	14.06	19.83
Copper (Cu)	0.91	0.70	2.37	8.57	23.85	25.38
Zinc (Zn)	1.87	1.89	4.56	9.90	8.24	12.90
Selenium (Se)	0.02	0.01	8.94	12.17	7.79	14.46
Bromine (Br)	0.03	0.02	3.93	8.50	4.49	9.62
Strontium (Sr)	0.11	0.08	3.57	9.63	23.53	25.46
Barium (Ba)	1.13	0.37	3.29	10.59	14.08	17.73
Arsenic (As)	–	0	6.97	10.17	3.53	10.77
Lead (Pb)	0.14	0.12	7.45	11.77	1.32	11.85

## 2.4 Blanks, LOD, and uncertainties

The limits of detection (LOD) based on blank levels obtained from Hi-Vol filter blanks ( $N > 40$ ), and various uncertainties, as well as overall uncertainties for all elements are given in Table 1. The concentration of blanks was calculated using Eq. (1) assuming 23 h sampling at  $1.13 \text{ m}^3 \text{ min}^{-1}$  and LOD was determined by 3 times the standard deviations of blanks. Values below LOD for S, K, Ca, Ti, Mn, Fe, Cu, Zn, As, Se, Br, Sr, Ba, and Pb were assigned as half of LOD values in all

the statistical analyses below. Other elements detected by the Xact, such as Sc (scandium), V (vanadium), Cr (chromium), Co (cobalt), Ni (nickel), Ge (germanium), Rb (rubidium), Ag (silver), Cd (cadmium), and Hg (mercury), for which  $> 50\%$  of aerosol samples were below the detection limits, are not included in the table or subsequent discussion. Calculation of uncertainties are discussed in Sect. 2.5. For most elements, overall uncertainties are less than 20%. Ti, Sr, and Cu have the highest uncertainties of 28, 25, and 25%, respectively.

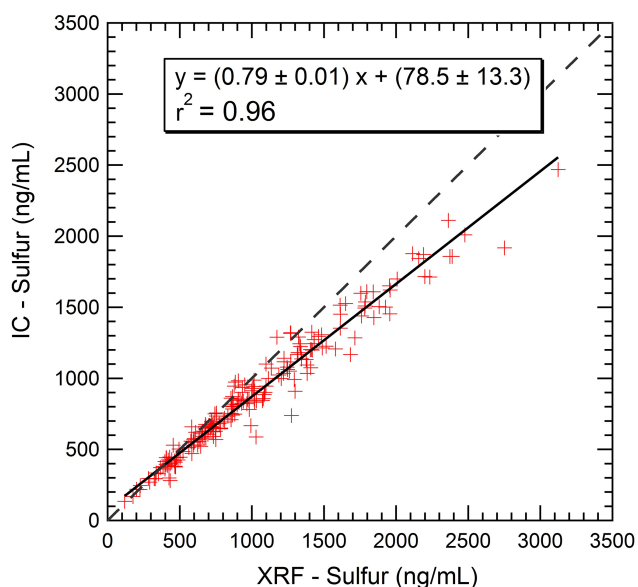


**Figure 3.** Sulfur measured by XRF and one-third of sulfate measured by IC (results of orthogonal regression are shown, along with 1 : 1 ratio by dotted line).

## 2.5 Source apportionment

A source apportionment analysis was performed with positive matrix factorization (PMF) (Paatero and Tapper, 1994) using EPA PMF 5.0 software. PMF analysis was applied on the combined data from JST (summer, fall, winter 2012, and spring 2013), GT (fall, winter 2012, and fall 2013), and RS (winter 2013 and fall 2013) (total  $N = 299$ ). Although the road-side site generally has higher levels of metals than the urban site (JST) and near-road site (GT) (discussed in Sect. 3.2.2), merging RS data with JST and GT in the analysis did not alter the PMF solutions substantially (factor profiles and source contributions), but the larger number of input data resulted in a more robust PMF solution. Fourteen elements (S, K, Ca, Ti, Mn, Fe, Cu, Zn, As, Se, Br, Sr, Ba, and Pb) and WSOC were run in the model with Ti and As categorized as weak species (low S/N signals). The concentrations, together with the uncertainties, were used as the input for PMF runs. Missing data were replaced by species median with 400 % uncertainty and values below LOD were assigned as half of LOD values with uncertainties of five-sixths the concentration (Polissar et al., 1998). For other data, uncertainties for each species were determined by multiplying the concentration by overall uncertainties (%). Overall uncertainty was calculated from the sum of square of various uncertainties including filter sampling (5 %), extraction (5 %), blanks ( $1\sigma$  of multiple blanks, 2–15 % depending on species), calibration ( $1\sigma$  of slope, 10 %), and analytical uncertainty. The analytical uncertainty for elements was obtained by analyzing the same sample, a composite of extracts from 11 selected road-side samples 20 times and calculating the coefficient of

variation (CV, %). The measured uncertainty for each element, based on two side-by-side Hi-Vol samplers at JST, was also included in the overall uncertainty. This was done because the calculated uncertainties for some elements (e.g., Cu and Sr) are much smaller than the measured uncertainties from collocated measurements (Table 1). By combining two uncertainties, the uncertainties for all elements are slightly overestimating. Uncertainty from collocated measurements was calculated as the relative uncertainty of the slope ( $1\sigma/\text{slope}$ ), which was based on an orthogonal regression (discussed below, see Fig. 4). Both uncertainties and the combined overall uncertainties for each element are given in Table 1. The PMF model was executed with 3–8 factors. Based on minimized  $Q$  values and physical interpretation of the solutions, a four-factor solution was found to be optimal. Details on determining the optimal factor and bootstrapping results can be found in the Supplement.

## 3 Results and discussions

### 3.1 Comparison with ion chromatography

As a further test of the system, sulfate concentrations were determined on a subset of the Hi-Vol filter samples by ion chromatography (IC) and compared to the elemental analysis of sulfur; 200 filters that included samples from JST and GT were extracted in DI water (same procedure discussed in Sect. 2.1, but without adding HNO<sub>3</sub> in the extracts), and inorganic sulfate (IC-sulfate) was measured by an ion chromatography (IC, DX500 with UTAC-ULP1 concentrator column, AG11 guard column, and AS11 anion column, DIONEX, CA). IC-sulfate was then divided by three to convert to sulfur mass (molar mass of sulfate and sulfur are 96 and 32 g mol<sup>-1</sup>, respectively) and directly compared to XRF-sulfur. Orthogonal regression shows good quantitative agreement and correlation coefficient ( $r^2$ ) of 0.96 (Fig. 3). The discrepancy between sulfur measured by XRF and IC (slope of IC-sulfur vs. XRF-sulfur =  $0.79 \pm 0.01$ ) may be attributed to roughly 20 % contributions from additional sulfur species, such as organosulfates that are not detected by the IC. Lower sulfur measured by IC versus XRF has also been observed in other studies (Shakya and Peltier, 2015; Tolocka and Turpin, 2012; He et al., 2001). However, Hidy et al. (2014) found no statistical evidence for organosulfates in the southeast by this difference method.

### 3.2 Water-soluble elements

#### 3.2.1 Inter-comparisons of two collocated Hi-Vols

Inter-comparisons of elements from two collocated Hi-Vol samplers ( $N = 11$ ) at JST in November 2012 are shown in Fig. 4, and results included in Table 1. Orthogonal regressions resulted in strong correlations for most elements ( $r^2 = 0.73$ – $0.99$ ) with moderate correlations for Cu ( $r^2 = 0.57$ )



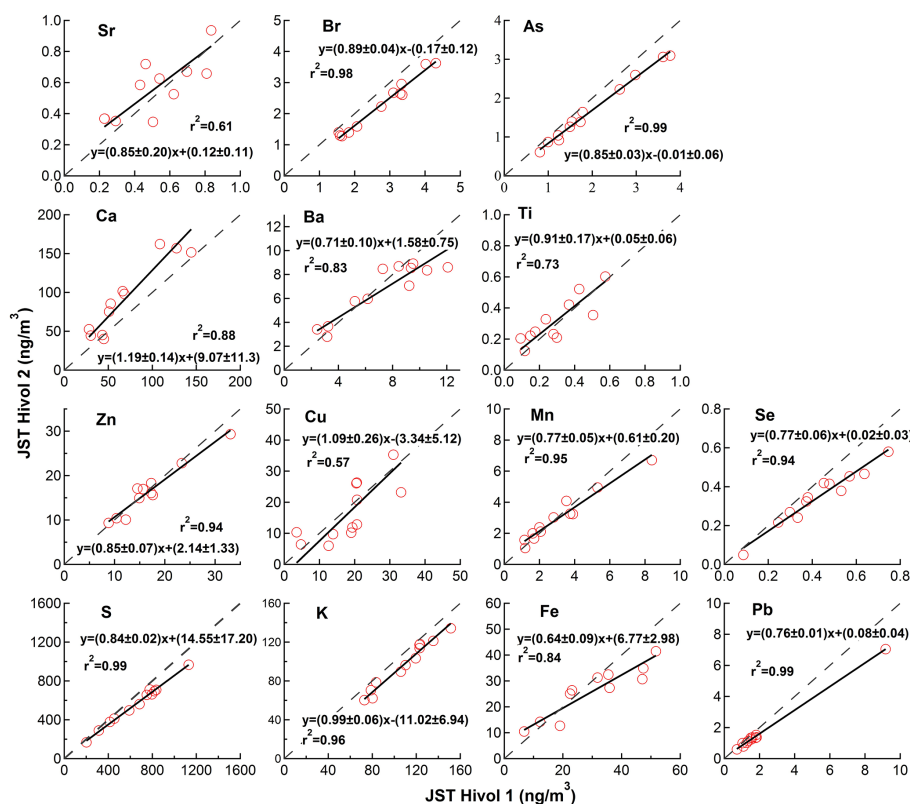


**Figure 4.** Precision from collocated measurements assessed by filter samples ( $N = 11$ ) collected simultaneously using two Hi-Vol samplers deployed at JST during November 2012 (analysis was done by orthogonal regression; the dotted line is 1 : 1).

and Sr ( $r^2 = 0.61$ ). The slopes show percentage differences (1-slope) are 1–10 % for Cu, K, and Ti, 11–20 % for S, Zn, Ca, Br, As, and Sr, and 20–36 % for Pb, Mn, Se, Fe, and Ba. Overall, the two Hi-Vols show good agreement for measuring water-soluble elements, considering the uncertainties from sampling, filter preparations, and extractions. The uncertainties in slope ( $1\sigma$ ) were used in calculating the overall uncertainties (Sect. 2.3). The intercepts were relatively small and thus ignored.

### 3.2.2 Spatial and temporal trends

Monthly average concentrations of water-soluble elements and WSOC at various sampling sites are given in Figs. 5 and Fig. S9, respectively. Three seasons (summer, fall, and winter) were grouped based on the temperature profiles in 2012 and 2013, consistent with our previous work (Fang et al., 2015a; Verma et al., 2014). As seen from Fig. 5, mass concentrations of water-soluble elements span a wide range, from  $0.1 \text{ ng m}^{-3}$  to  $1.2 \mu\text{g m}^{-3}$ . S is the most abundant water-soluble element of the group measured, comprising  $71 \pm 14\%$  of the total measured element mass. Ca, K, Fe, Cu, Zn, and Ba follow with average ( $\pm 1\sigma$ ) fractions of 16 ( $\pm 12$ )%, 8 ( $\pm 5$ )%, 1.8 ( $\pm 1.3$ )%, 1.4 ( $\pm 2.1$ )%, 1.4 ( $\pm 1.4$ )%, and 0.5 ( $\pm 0.6$ )%.

Seasonal variability of all elements can be examined from the Atlanta urban sites (JST, GT, and RS). Besides S, commonly found to have higher concentration in summer due to the higher SO<sub>2</sub> oxidation rates in warm seasons (Hidy et al., 2014), most of the water-soluble elements also had higher concentrations in summer/fall, such as Ca, Fe, Cu, Mn, Sr, and Se. The seasonal variability of these elements may be explained by different causes: elevated concentration of some elements (Ca, Mn, and Sr) may be attributed to drier conditions in summer favoring the re-suspension of mineral dust; Cu and Fe may be related to secondary formation (discussed in the source apportionment in Sect. 3.2.3); and Se is likely due to its coal combustion origins (Bell et al., 2007), thus following a similar trend as S. In contrast, K can be associated with both biomass burning and mineral dust (Zhang et al., 2010; Hueglin et al., 2005) (discussed below and Fig. S3 in the Supplement) and has less seasonal variability, with only slightly higher concentrations in winter due to more biomass burning during that period. Other metals (Zn, Ba, Br, Pb, Ti, and As) do not exhibit apparent seasonal trends.

Spatial variability of water-soluble elements is important in assessing human exposure, within/across cities, for epidemiological studies, and provides insights on sources. The BHM site has high ambient concentration of most water-soluble metals, such as Mn, Zn, and Pb, with respect to other

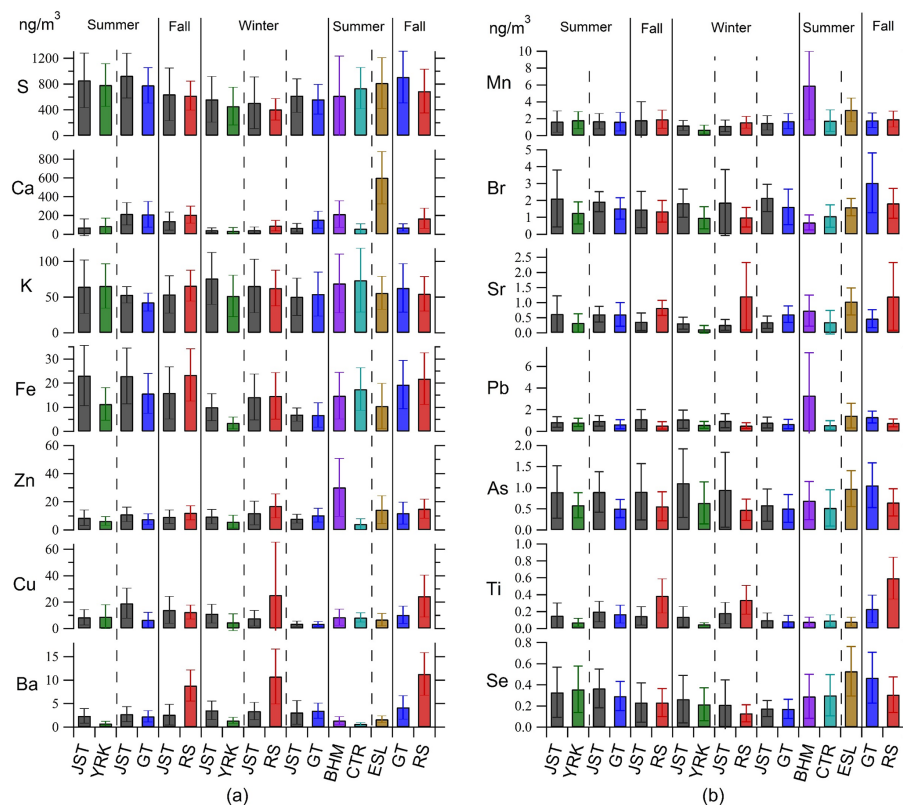


**Figure 5.** Monthly mean ( $\pm$  standard deviation) of water-soluble elements ambient concentration ( $\text{ng m}^{-3}$ ) at various sampling sites. Seasons are separated by solid lines and simultaneous sampling at paired sites are separated by dashed lines (urban – JST, BHM, ESL; rural – YRK, CTR; near-road – GT; road-side – RS).

sites, pointing to industrial sources for these metals in this urban environment. The ratio of averaged Mn, Zn, and Pb at BHM to its paired rural site CTR is 3.3, 7.0, and 5.7, respectively. ESL, an urban site also strongly impacted by numerous industrial sources (Bae et al., 2006), has the highest Ca and Se concentrations among all sites, and higher Mn and Pb than all Atlanta sites (JST, GT, RS, and YRK). Among the four sites in Atlanta, there was a distinct relationship between the concentration of water-soluble elements and distance to traffic sources. Generally, the road-side (RS) site had much higher element concentrations relative to the rural YRK site, which had notably low concentrations of Cu, Ba, Sr and Ti. For example, the ratio of averaged Cu, Ba, Sr, and Ti at RS to its paired Atlanta urban JST site, is 0.9, 3.4, 2.2, and 2.6, respectively, in fall and 3.3, 3.1, 4.6, and 1.9 in winter. Comparing RS to the near-road GT site, ratios are 2.2, 2.7, 2.5 and 2.6 in fall for Cu, Ba, and Ti. Concentrations at YRK were typically much lower than the paired JST urban site, both in summer (ratio of average concentration YRK/JST = 1.1, 0.3, 0.5, and 0.5) and winter (0.4, 0.4, 0.4, and 0.3) for Cu, Ba, Sr and Ti, respectively.

To further explore the spatial heterogeneity of water-soluble elements in Atlanta and the surrounding region, the coefficient of divergence (COD) (Wilson et al., 2005) and

correlation coefficient (Pearson's  $r$ ) were calculated for each paired site for all elements. A COD close to 0 represents a homogenous distribution, and near 1 indicates heterogeneity. Both are summarized in Table S2 (Supplement), and  $r$  values are shown in Fig. 6. The COD and correlation coefficient ( $r$ ) for WSOC were also included in Table S2 in the Supplement.

JST and GT are in close proximity. These two sites had the most similar concentrations for many water-soluble elements, with  $r$  ranging from 0.71 to 0.98 and relatively low CODs (0.06–0.20), except for Cu and Ti. In summer Cu measured at JST and GT have a moderate correlation ( $r = 0.68$ ) but high COD (0.52), with much higher concentration at JST (mean =  $19.1 \text{ ng m}^{-3}$ , median =  $18.5 \text{ ng m}^{-3}$ ) than GT (mean =  $6.6 \text{ ng m}^{-3}$ , median =  $5.1 \text{ ng m}^{-3}$ ). In winter, although the average values are similar ( $3.7$  and  $3.6 \text{ ng m}^{-3}$  for JST and GT, respectively), there is no correlation ( $r = -0.06$ ) and COD is fairly high (0.35). Ti between the two sites have low correlations ( $r = 0.48$  in summer and  $0.51$  in winter) and high COD (0.38 and 0.36 in summer and winter, respectively).

For the urban/rural (JST/YRK) pair, S, K, Ca, Mn, and Se tended to co-vary and have similar concentrations at the urban and rural sites, pointing to a more regional characteristic (sources) for these elements. The other elements did not



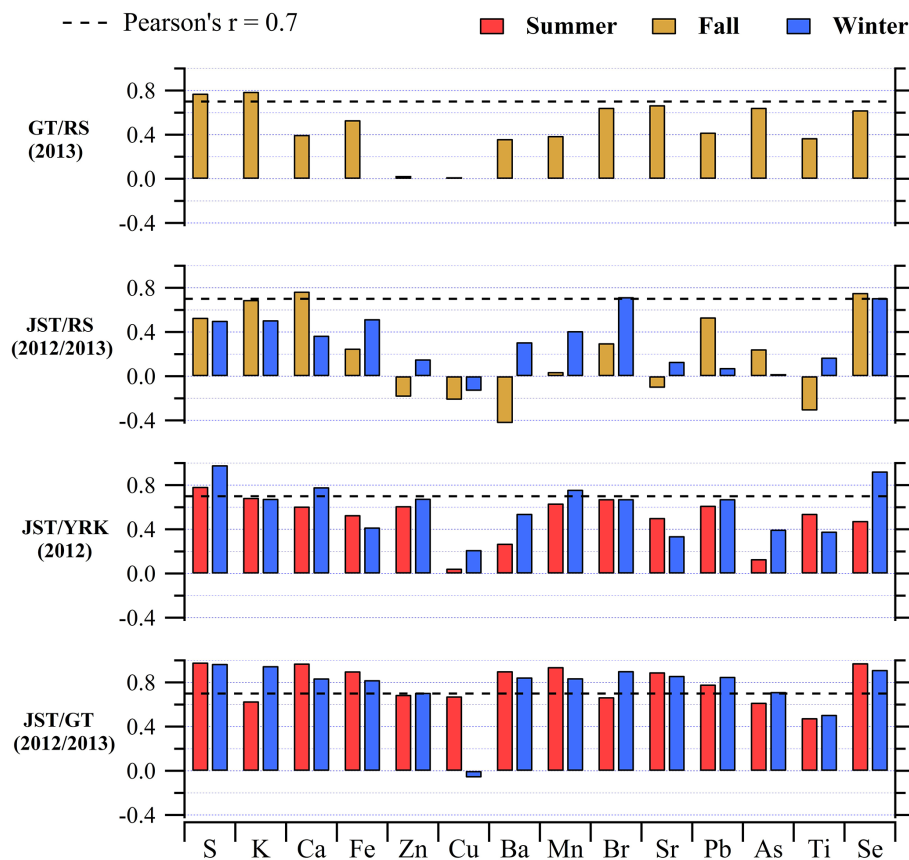


**Figure 6.** Correlations (Pearson's  $r$ ) between paired sites for various water-soluble elements in Georgia (JST, RS, GT, and YRK).

co-vary at these two sites and are generally higher at the urban site (JST).

Comparison of the road-side site (RS) to the representative urban site (JST) provides insights into which elements are associated with traffic emissions and how they vary with season. S and K were not correlated well between JST and RS in both fall and winter, suggesting the presence of other local sources for S and K at the RS site, for example re-suspended dust (Minguillón et al., 2014; Hueglin et al., 2005). For Cu, Ba, Sr and Ti, the high COD ( $> 0.4$ ), low  $r$  values ( $r < 0.3$ ) between various paired sites, and their concentrations highest at RS, are all indicators of emissions associated with traffic as a dominant source (Fig. 5).

### 3.2.3 Source apportionment

PMF was applied to the combined data from JST, GT, and RS (total  $N = 299$ ), and four factors were resolved. They are labeled brake/tire wear, biomass burning, secondary formation, and mineral dust, based on the loading of specific elements identified as various source tracers. Note, metals as source tracers are typically based on total metals, whereas here we are using the measured water-soluble concentrations. Factor profiles and time series plots (from the JST site) are

shown in Fig. 7a and b, respectively. The percentage contribution of the various factors (sources) to the four important health-related metals (Cu, Fe, Zn, and Mn) is shown in Fig. 8. Breakdown of sources for the other water-soluble elements and WSOC can be found in Fig. S3 in the Supplement.

The factor with high loadings for Ti, Fe, Cu, Zn, and Ba is identified as a brake/tire wear source as it includes products from brake pads or linings, such as Cu (Adachi and Tainosho, 2004; Sternbeck et al., 2002; Garg et al., 2000), Fe (Adachi and Tainosho, 2004; Garg et al., 2000; Hopke et al., 1980), Ti (Adachi and Tainosho, 2004), and Zn (Adachi and Tainosho, 2004; Sternbeck et al., 2002), and tracers of tire wear, e.g., Zn (Harrison et al., 2012). A biomass burning factor is identified by high concentrations of K, Br, As, and Pb. While K is a typical component in biomass burning aerosols, Br (Turn et al., 1997) and Pb (Richard et al., 2011) have also been found in wood combustion. The time series plot (Fig. 7b) showed a higher contribution of this factor in winter than in summer (winter<sub>avg</sub>/summer<sub>avg</sub>  $\approx 1.35$ ), consistent with the observed winter enhancement of biomass burning emissions in Atlanta (Zhang et al., 2010). Some water-soluble metals (e.g., Se, Fe, Br, Pb, As, Mn, Ba, and Zn) were apportioned to the biomass burning factor (see Figs. 8 and S3 in the Supplement). The total form of some of these metals (Fe,

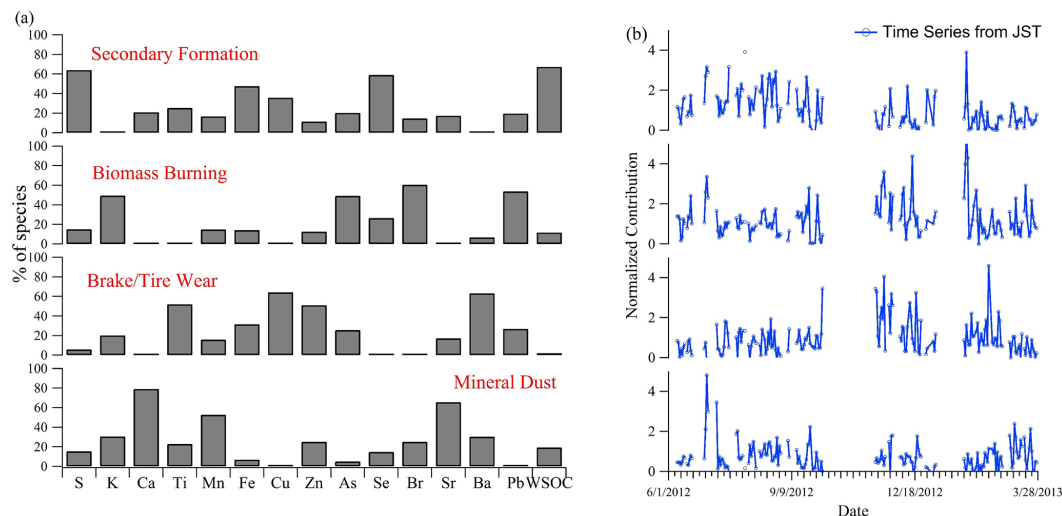


**Figure 7.** Loading of measured water-soluble elements into various PMF resolved factors for all Atlanta sites (a) and factor time series of source contributions resolved from the Jefferson Street Site (JST, urban Atlanta) (b).

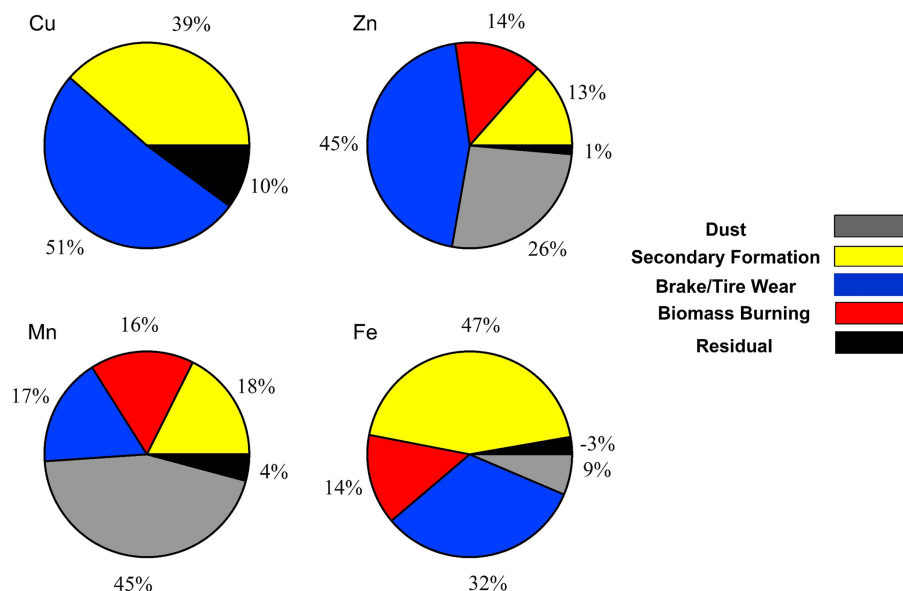


**Figure 8.** Factor contributions for water-soluble Cu, Zn, Mn, and Fe in PM<sub>2.5</sub> based on the PMF analyses.

Mn, Zn, and Cu) (Chang-Graham et al., 2011) and water-soluble Fe have been seen in biomass burning in other studies (Oakes et al., 2012). The third factor, referred to as secondary formation, is characterized by high S, WSOC, and Se, and some Fe, with higher contributions in summer than winter ( $\text{summer}_{\text{avg}}/\text{winter}_{\text{avg}} \approx 2.37$ ). For the last source, a mineral dust origin is suggested by high loadings of Ca, Mn, and Sr, all indicators of crustal material. The results have implications for health studies.

### 3.2.4 Redox-active transition metals: Cu, Fe, and Mn

A number of studies have linked water-soluble redox-active Cu, Fe, and Mn to reactive oxygen species (Cheung et al., 2012, 2010; Kam et al., 2011; Shen and Anastasio, 2011; Akhtar et al., 2010; Landreman et al., 2008; Zhang et al., 2008; Kodavanti et al., 2005). After S, K, and Ca, these metals (i.e., water-soluble Cu, Fe, and Mn) generally have higher ambient concentrations than other measured elements (Fig. 5). In addition, Cu and Mn are thought to make major contributions to particle-catalyzed ROS generation (e.g., DTT (dithiothreitol) assay (Charrier and Anastasio, 2012)).

Exploring the sources of the water-soluble fractions of these metals is pertinent to our health studies.

As shown in Fig. 8, tire/brake wear is the dominant source for Cu (51 %). It is also strongly correlated with Ba ( $r = 0.70$ – $0.84$ , Table S3 in the Supplement) at the road-side site (RS), and Ba is a good indicator for a brake lining source (Gietl et al., 2010; Torre et al., 2002). The other important contributor to Cu is secondary formation (39 %).

Although Zn is not redox-active, we include it here in the discussion since it was also significantly loaded in the tire/brake wear factor (45 %) and has been linked to adverse health effects (Akhtar et al., 2010; Kodavanti et al., 2005). PMF analyses suggests that Zn has additional sources, with 26 % associated with the mineral dust factor, 14 % with the biomass burning, and 13 % with secondary formation. Zn is also correlated with other water-soluble metals, to various degrees (Fe, Pb, Mn, Sr, K, Ca, Ti, and Cu with  $r$  ranging from 0.70 to 0.89, Table S3 in the Supplement).

Overall, the results (Fig. 8) show that brake/tire wear is an important traffic source for Cu (51 %), Fe (32 %), Mn (17 %), and Zn (45 %). Studies have specifically linked these metals from brake wear, or traffic sources in general, to pro-inflammatory responses (e.g., Gasser et al., 2009) and observed adverse health responses (e.g., Riediker et al., 2004). Combined with engine combustion emissions, which includes many organic components (e.g., quinones), the large fraction of water-soluble Cu, along with contributions from Fe and Mn from brake/tire wear, make mobile source emissions important ROS sources (Bates et al., 2015). In contrast, these redox-active metals are not found at significant levels in the biomass burning factor (Fig. 7), which has been found to be a contributor to the PM<sub>2.5</sub> DTT activity in the SCAPE study (Verma et al., 2014, 2015; Bates et al., 2015), indicating that redox-active organic species dominate in that case.

The major identified source for Mn is mineral dust (45 %) with other sources making relatively similar contributions: secondary formation (18 %), biomass burning (16 %), and brake/tire wear (17 %). At YRK, the rural site least affected by traffic, Mn correlates best with Ca ( $r = 0.91$ ) and Sr ( $r = 0.82$ , Table S3) in summer and K ( $r = 0.86$ ), Ca ( $r = 0.86$ ), Zn ( $r = 0.89$ ), and Sr ( $r = 0.79$ ) in winter, all indicative of regional mineral dust contributions, consistent with the regional characteristic of Mn discussed in Sect. 3.2.2.

For Fe, besides the brake/tire factor, a large fraction (47 %) is apportioned to the secondary formation factor, and Fe correlates well with S at JST ( $r = 0.71$ ), YRK ( $r = 0.76$ ), and GT ( $r = 0.73$ ) in summer, and at JST ( $r = 0.76$ ) in fall 2012 and RS ( $r = 0.74$ ) in fall 2013. Fe and S are moderately correlated at RS in fall 2012 ( $r = 0.62$ ), and GT ( $r = 0.55$ ) in fall 2013. The highest correlations occur when secondary atmospheric processing (oxidation) is strong. These results are consistent with a previous study involving single particle chemical analysis on PM<sub>2.5</sub> particles in Atlanta, which showed that sulfate is an important proxy for Fe solubility (Oakes et al., 2012) by affecting aerosol pH, or as an indi-

cator of iron sulfates, which are soluble and possibly formed at some point earlier in the particles lifespan under acidic conditions. Metal mobilization by formation of an aqueous particle with secondary acids may also explain the important contribution of secondary formation (39 %) to Cu in the southeastern USA, although the correlations between Cu and S were weaker compared to those between Fe and S (Cu – S  $r = 0.51$ , 0.09, and 0.66 at JST, YRK, and GT in summer, respectively, Table S3). The correlation between S and water-soluble Fe and Cu might explain past associations found in other studies between sulfate/sulfur oxide and health endpoints (Atkinson et al., 2010; Sarnat et al., 2008; Pope et al., 2002; Gwynn et al., 2000; Dockery et al., 1996; Raizenne et al., 1996).

PM<sub>2.5</sub> mass is regulated and has been associated with adverse health endpoints in many studies (Laden et al., 2000; Pope et al., 2002, 2004; Metzger et al., 2004; Sarnat et al., 2008). Overall, water-soluble iron was highly correlated with PM<sub>2.5</sub> mass ( $r = 0.73$ – $0.80$ , Table S4), due to a correlation with sulfate (e.g., role of sulfate on aerosol pH). Interestingly, Fe was correlated with PM<sub>2.5</sub> mass even in some cases when S did not co-vary with PM<sub>2.5</sub> concentration. These cases are all in winter when the  $r$  values between PM<sub>2.5</sub> mass and S were 0.52, 0.35, 0.26, and 0.23, while those with Fe were 0.80, 0.75, 0.76, and 0.74 at JST (December), JST (March), GT (March), and RS (February), respectively. The exceptions were the two rural sites (YRK and CTR), where water-soluble Fe was moderately or not correlated with PM<sub>2.5</sub> at all ( $r = 0.69$  at YRK  $r = 0.3$  at CTR) while S and PM<sub>2.5</sub> still had high correlations ( $r = 0.78$  and 0.75 at YRK and CTR respectively).

Mn and Zn show some correlations with PM<sub>2.5</sub> mass as well, but only during two periods (for Mn,  $r = 0.84$  at GT and 0.76 at RS, both in winter, for Zn,  $r = 0.71$  and 0.76 at JST in December and March, respectively). No significant correlations were ever found between PM<sub>2.5</sub> and Cu. It has been demonstrated that water-soluble metals (Zn, Cu, and Fe) can have adverse effects on the respiratory system and our observations suggest that some water-soluble metals, especially Fe, are correlated with PM<sub>2.5</sub> mass. However, some epidemiological studies point to organic carbon (Peel et al., 2005; Metzger et al., 2004) and PM<sub>2.5</sub> mass (Sarnat et al., 2008; Pope et al., 2004; Metzger et al., 2004; Pope et al., 2002; Laden et al., 2000) but not metals. Li et al. (2009) suggests that redox-active organic chemicals could play major roles in PM toxicity and metals may synergize with organic PM components to further escalate oxidative stress. Thus, these water-soluble metals could play both dominant and important secondary roles in driving observed associations between fine particles and adverse health.

## 4 Conclusions

Over 500 PM<sub>2.5</sub> filter samples (23hr integration time) were collected during 2012–2013 at multiple sites (three urban, two rural, one near-road site, and one road-side site) in the southeastern United States, using paired (simultaneous measurements at two different sites) high-volume samplers, as part of the Southeastern Center for Air Pollution & Epidemiology (SCAPE) project. A focus of SCAPE was assessing the role of PM<sub>2.5</sub> associated reactive oxygen species (ROS) on health effects. Because water-soluble metals have been linked to ROS, a method was developed to measure the water-soluble elements (S, K, Ca, Ti, Mn, Fe, Cu, Zn, As, Se, Br, Sr, Ba, and Pb) on filters that were also analyzed for aerosol ROS activity by various assays (i.e., DTT and AA assays, discussed in other publications: Fang et al., 2015a, b; Verma et al., 2014). Water-soluble elements were determined by extracting filters in deionized water, re-aerosolizing the extracts and directing to an instrument designed for on-line measurements of aerosol elemental composition by non-destructive X-ray fluorescence. The system response was calibrated with standard solutions of multiple elements, which were also used as positive controls when running ambient samples to ensure stability and reproducibility (coefficient of variation < 10 %). The method LOD (limit of detection) for each element was reasonably low (< 25 % of typical sample levels), and the overall uncertainties were less than 20 % for most elements, except for Cu, Sr, and Ti, with overall relative uncertainties of 25, 25, and 28 %, respectively. The method was further validated by comparing with sulfate measured by ion chromatography on the same ambient filter samples.

Water-soluble elements spanned a wide range of concentrations, from LODs (typically 0.1–30 ng m<sup>-3</sup>) to 1.2 µg m<sup>-3</sup>, with S as the most abundant element, followed by Ca, K, Fe, Cu, Zn, and Ba. Positive matrix factorization (PMF) was used for source apportionment analyses. Four factors were identified: brake/tire wear, characterized by Ba, Zn, Cu, and Ti; biomass burning, characterized by K and Br; secondary formation, characterized by S, Se, Fe, and WSOC; and mineral dust, characterized by Ca, Mn, and Sr. Elements associated with secondary formation and mineral dust were higher during warm/dry seasons when aerosol re-suspension is favored (water-soluble Ca, Mn, and Sr) and secondary formation is high (water-soluble Fe and Cu). S and Se, products from coal combustion, were also at higher concentration in summer compared to winter. K had only slightly higher concentrations in winter due to contributions from biomass burning (mainly winter) and mineral dust emissions (mainly summer). Other elements (Zn, Ba, Br, Pb, Ti, and As) did not exhibit seasonal trends. Spatially, S, K, Ca, Mn, and Se were generally homogeneously distributed, while Cu, Ba, Sr and Ti were more heterogeneously distributed, with highest levels near roadways. The other two urban sites outside of Georgia were heavily impacted by industrial sources, contributing to

higher concentration of Zn, Mn, and Pb at Birmingham, AL (BHM), and Ca and Se at the East St. Louis, IL (ESL) site.

The redox-active metals, Cu, Mn, and Fe have been linked to ROS and oxidative stress. Among the four PMF factors, brake/tire wear contributed most to the water-soluble form of these elements in this study, with 51 % for Cu, 32 % for Fe, and 17 % for Mn, pointing to the importance of this source in contributing to fine particle ROS activity. Organic compounds from combustion also contribute to ROS activity, making overall vehicle emissions important sources of PM<sub>2.5</sub> ROS.

Mn was associated mainly with mineral dust (45 %). Water-soluble Zn, a redox-inactive metal, but often identified as toxic in health studies, and among the highest in concentration in this study, was associated with a mixture of factors (45 % brake/tire wear, 26 % mineral dust, 14 % biomass burning, and 13 % secondary formation).

Roughly 50 % of water-soluble Fe was associated with the secondary formation factor, and was highly correlated with S (Pearson's  $r = 0.71$ – $0.76$ ). There was also substantial loading of Cu (39 %) in this factor. Our previous studies in the southeast have linked water-soluble Fe (measured by a different technique) to sulfate, aerosol pH and soluble iron sulfates (Oakes et al., 2012). The association of Cu with this factor could also be due to increased solubility by sulfur-driven aerosol acidity. Of the four water-soluble metals (Cu, Mn, Fe, and Zn), only Fe was correlated with PM<sub>2.5</sub> mass ( $r = 0.73$ – $0.80$ ), due to its association with S. We have previously reported that ROS (DTT assay) measured on these same filters was correlated with PM<sub>2.5</sub> mass (Fang et al., 2015a). These results indicate that additional aerosol components, such as redox-active organic compounds (Verma et al., 2015, 2014, 2012) also play a significant role in the ROS activity of aerosols in the southeastern USA, in addition to these water-soluble metals.

**The Supplement related to this article is available online at doi:10.5194/acp-15-11667-2015-supplement.**

*Acknowledgements.* This publication was made possible by US EPA grant R834799. The contents are solely the responsibility of the grantee and do not necessarily represent the official views of the US EPA. Further, US EPA does not endorse the purchase of any commercial products or services mentioned in the publication. The authors thank Laura King for assistance in collecting samples, R. Erik Weber and Janessa Riana Rowland for assistance in lab work and the SEARCH personnel for their many contributions supporting the field deployments. T. Fang acknowledges the support from the Oversea Study Program of Guangzhou Elite Project.

Edited by: F. Keutsch

## References

- Adachi, K. and Tainosho, Y.: Characterization of heavy metal particles embedded in tire dust, *Environ. Int.*, 30, 1009–1017, doi:10.1016/j.envint.2004.04.004, 2004.
- Akhtar, U. S., McWhinney, R. D., Rastogi, N., Abbatt, J. P. D., Evans, G. J., and Scott, J. A.: Cytotoxic and proinflammatory effects of ambient and source-related particulate matter (PM) in relation to the production of reactive oxygen species (ROS) and cytokine adsorption by particles, *Inhalation Toxicol.*, 22, 37–47, doi:10.3109/08958378.2010.518377, 2010.
- Atkinson, R. W., Fuller, G. W., Anderson, H. R., Harrison, R. M., and Armstrong, B.: Urban ambient particle metrics and health: a time-series analysis, *Epidemiology*, 21, 501–511, doi:10.1097/EDE.0b013e3181debc88, 2010.
- Bae, M.-S., Schauer, J. J., and Turner, J. R.: Estimation of the monthly average ratios of organic mass to organic carbon for fine particulate matter at an urban site, *Aerosol Sci. Technol.*, 40, 1123–1139, doi:10.1080/02786820601004085, 2006.
- Bates, J. T., Weber, R. J., Abrams, J., Verma, V., Fang, T., Klein, M., Strickland, M. J., Sarnat, S. E., Chang, H. H., Mulholland, J. A., Tolbert, P. E., and Russell, A. G.: Reactive Oxygen Species Generation Linked to Sources of Atmospheric Particulate Matter and Cardiorespiratory Effects, *Environ. Sci. Technol.*, accepted, doi:10.1021/acs.est.5b02967, 2015.
- Bell, M. L., Dominici, F., Ebisu, K., Zeger, S. L., and Samet, J. M.: Spatial and temporal variation in PM(2.5) chemical composition in the United States for health effects studies, *Environ. Health Perspect.*, 115, 989–995, doi:10.1289/ehp.9621, 2007.
- Birmili, W., Allen, A. G., Bary, F., and Harrison, R. M.: Trace Metal Concentrations and Water Solubility in Size-Fractionated Atmospheric Particles and Influence of Road Traffic, *Environ. Sci. Technol.*, 40, 1144–1153, doi:10.1021/es0486925, 2006.
- Brunekreef, B., Janssen, N. A., de Hartog, J., Harssema, H., Knape, M., and van Vliet, P.: Air pollution from truck traffic and lung function in children living near motorways, *Epidemiology*, 8, 298–303, doi:10.1097/00001648-199705000-00012, 1997.
- Burchiel, S. W., Lauer, F. T., Dunaway, S. L., Zawadzki, J., McDonald, J. D., and Reed, M. D.: Hardwood smoke alters murine splenic T cell responses to mitogens following a 6-month whole body inhalation exposure, *Toxicol. Appl. Pharmacol.*, 202, 229–236, doi:10.1016/j.taap.2004.06.024, 2005.
- Burnett, R. T., Brook, J., Dann, T., Delocla, C., Philips, O., Cakmak, S., Vincent, R., Goldberg, M. S., and Krewski, D.: Association between particulate- and gas-phase components of urban air pollution and daily mortality in eight Canadian cities, *Inhal. Toxicol.*, 12, 15–39, doi:10.1080/08958370050164851, 2000.
- Chang-Graham, A. L., Profeta, L. T. M., Johnson, T. J., Yokelson, R. J., Laskin, A., and Laskin, J.: Case study of water-soluble metal containing organic constituents of biomass burning aerosol, *Environ. Sci. Technol.*, 45, 1257–1263, doi:10.1021/es103010j, 2011.
- Charrier, J. G. and Anastasio, C.: On dithiothreitol (DTT) as a measure of oxidative potential for ambient particles: evidence for the importance of soluble transition metals, *Atmos. Chem. Phys.*, 12, 9321–9333, doi:10.5194/acp-12-9321-2012, 2012.
- Cheung, K., Shafer, M. M., Schauer, J. J., and Sioutas, C.: Diurnal trends in oxidative potential of coarse particulate matter in the Los Angeles basin and their relation to sources and chemical composition, *Environ. Sci. Technol.*, 46, 3779–3787, doi:10.1021/es204211v, 2012.
- Cheung, K. L., Ntziachristos, L., Tzamkiozis, T., Schauer, J. J., Samaras, Z., Moore, K. F., and Sioutas, C.: Emissions of particulate trace elements, metals and organic species from gasoline, diesel, and biodiesel passenger vehicles and their relation to oxidative potential, *Aerosol Sci. Technol.*, 44, 500–513, doi:10.1080/02786821003758294, 2010.
- Chevion, M.: A site-specific mechanism for free radical induced biological damage: The essential role of redox-active transition metals, *Free Radical Biol. Medicine*, 5, 27–37, doi:10.1016/0891-5849(88)90059-7, 1988.
- Cho, W.-S., Duffin, R., Poland, C. A., Duschl, A., Oostingh, G. J., MacNee, W., Bradley, M., Megson, I. L., and Donaldson, K.: Differential pro-inflammatory effects of metal oxide nanoparticles and their soluble ions in vitro and in vivo; zinc and copper nanoparticles, but not their ions, recruit eosinophils to the lungs, *Nanotoxicology*, 6, 22–35, doi:10.3109/17435390.2011.552810, 2011.
- Darrow, L. A., Klein, M., Flanders, W. D., Waller, L. A., Correa, A., Marcus, M., Mulholland, J. A., Russell, A. G., and Tolbert, P. E.: Ambient air pollution and preterm birth: a time-series analysis, *Epidemiology*, 20, 689–698, doi:10.1097/EDE.0b013e3181a7128f, 2009.
- Darrow, L. A., Klein, M., Strickland, M. J., Mulholland, J. A., and Tolbert, P. E.: Ambient air pollution and birth weight in full-term infants in Atlanta, 1994–2004, *Environ. Health Perspect.*, 119, 731–737, doi:10.1289/ehp.1002785, 2011.
- Dockery, D. W., Cunningham, J., Damokosh, A. I., Neas, L. M., Spengler, J. D., Koutrakis, P., Ware, J. H., Raizenne, M., and Speizer, F. E.: Health effects of acid aerosols on North American children: respiratory symptoms, *Environ. Health Perspect.*, 104, 500–505, 1996.
- Espinosa, A. J. F., Rodríguez, M. T., de la Rosa, F. J. B., and Sánchez, J. C. J.: A chemical speciation of trace metals for fine urban particles, *Atmos. Environ.*, 36, 773–780, doi:10.1016/S1352-2310(01)00534-9, 2002.
- Fang, T., Verma, V., Guo, H., King, L. E., Edgerton, E. S., and Weber, R. J.: A semi-automated system for quantifying the oxidative potential of ambient particles in aqueous extracts using the dithiothreitol (DTT) assay: results from the Southeastern Center for Air Pollution and Epidemiology (SCAPE), *Atmos. Meas. Tech.*, 8, 471–482, doi:10.5194/amt-8-471-2015, 2015a.
- Fang, T., Verma, V., Bates, J. T., Abrams, J., Klein, M., Strickland, M. J., Sarnat, S. E., Chang, H. H., Mulholland, J. A., Tolbert, P. E., Russell, A. G., and Weber, R. J.: Oxidative Potential of Ambient Water-Soluble PM<sub>2.5</sub> Measured by Dithiothreitol (DTT) and Ascorbic Acid (AA) Assays in the Southeastern United States: Contrasts in Sources and Health Associations, *Atmos. Chem. Phys.*, in preparation, 2015b.
- Garg, B. D., Cadle, S. H., Mulawa, P. A., Groblicki, P. J., Laroo, C., and Parr, G. A.: Brake wear particulate matter emissions, *Environ. Sci. Technol.*, 34, 4463–4469, doi:10.1021/es001108h, 2000.
- Gasser, M., Riediker, M., Mueller, L., Perrenoud, A., Blank, F., Gehr, P., and Rothen-Rutishauser, B.: Toxic effects of brake wear particles on epithelial lung cells in vitro, *Particle Fibre Toxicol.*, 6, 30, doi:10.1186/1743-8977-6-30, 2009.



- Gietl, J. K., Lawrence, R., Thorpe, A. J., and Harrison, R. M.: Identification of brake wear particles and derivation of a quantitative tracer for brake dust at a major road, *Atmos. Environ.*, 44, 141–146, doi:10.1016/j.atmosenv.2009.10.016, 2010.
- Gwynn, R. C., Burnett, R. T., and Thurston, G. D.: A time-series analysis of acidic particulate matter and daily mortality and morbidity in the Buffalo, New York, region, *Environ. Health Perspect.*, 108, 125–133, 2000.
- Hansen, D. A., Edgerton, E. S., Hartsell, B. E., Jansen, J. J., Kandasamy, N., Hidy, G. M., and Blanchard, C. L.: The Southeastern aerosol research and characterization study: Part 1 – Overview, *J. Air Waste Manag. Assoc.*, 53, 1460–1471, doi:10.1080/10473289.2003.10466318, 2003.
- Harrison, R. M., Jones, A. M., Gietl, J., Yin, J., and Green, D. C.: Estimation of the contributions of brake dust, tire wear, and resuspension to nonexhaust traffic particles derived from atmospheric measurements, *Environ. Sci. Technol.*, 46, 6523–6529, doi:10.1021/es300894r, 2012.
- He, K., Yang, F., Ma, Y., Zhang, Q., Yao, X., Chan, C. K., Cadle, S., Chan, T., and Mulawa, P.: The characteristics of PM<sub>2.5</sub> in Beijing, China, *Atmos. Environ.*, 35, 4959–4970, doi:10.1016/S1352-2310(01)00301-6, 2001.
- Heal, M. R., Hibbs, L. R., Agius, R. M., and Beverland, I. J.: Total and water-soluble trace metal content of urban background PM<sub>10</sub>, PM<sub>2.5</sub> and black smoke in Edinburgh, UK, *Atmos. Environ.*, 39, 1417–1430, doi:10.1016/j.atmosenv.2004.11.026, 2005.
- Hidy, G. M., Blanchard, C. L., Baumann, K., Edgerton, E., Tanenbaum, S., Shaw, S., Knipping, E., Tombach, I., Jansen, J., and Walters, J.: Chemical climatology of the southeastern United States, 1999–2013, *Atmos. Chem. Phys.*, 14, 11893–11914, doi:10.5194/acp-14-11893-2014, 2014.
- Hopke, P. K., Lamb, R. E., and Natusch, D. F. S.: Multielemental characterization of urban roadway dust, *Environ. Sci. Technol.*, 14, 164–172, doi:10.1021/es60162a006, 1980.
- Huang, Y. C., Ghio, A. J., Stonehuerner, J., McGee, J., Carter, J. D., Grambow, S. C., and Devlin, R. B.: The role of soluble components in ambient fine particles-induced changes in human lungs and blood, *Inhal. Toxicol.*, 15, 327–342, doi:10.1080/089583703044460, 2003.
- Hueglin, C., Gehrig, R., Baltensperger, U., Gysel, M., Monn, C., and Vonmont, H.: Chemical characterisation of PM<sub>2.5</sub>, PM<sub>10</sub> and coarse particles at urban, near-city and rural sites in Switzerland, *Atmos. Environ.*, 39, 637–651, doi:10.1016/j.atmosenv.2004.10.027, 2005.
- Kam, W., Ning, Z., Shafer, M. M., Schauer, J. J., and Sioutas, C.: Chemical characterization and redox potential of coarse and fine particulate matter (PM) in underground and ground-level rail systems of the Los Angeles metro, *Environ. Sci. Technol.*, 45, 6769–6776, doi:10.1021/es201195e, 2011.
- Kleinman, M. T., Sioutas, C., Froines, J. R., Fanning, E., Hamade, A., Mendez, L., Meacher, D., and Oldham, M.: Inhalation of concentrated ambient particulate matter near a heavily trafficked road stimulates antigen-induced airway responses in mice, *Inhal. Toxicol.*, 19, 117–126, doi:10.1080/08958370701495345, 2007.
- Kodavanti, U. P., Schladweiler, M. C., Ledbetter, A. D., McGee, J. K., Walsh, L., Gilmour, P. S., Highfill, J. W., Davies, D., Pinkerton, K. E., Richards, J. H., Crissman, K., Andrews, D., and Costa, D. L.: Consistent pulmonary and systemic responses from inhalation of fine concentrated ambient particles: roles of rat strains used and physicochemical properties, *Environ. Health Perspect.*, 113, 1561–1568, doi:10.1289/ehp.7868, 2005.
- Laden, F., Neas, L. M., Dockery, D. W., and Schwartz, J.: Association of fine particulate matter from different sources with daily mortality in six U.S. cities, *Environ. Health Perspect.*, 108, 941–947, doi:10.2307/3435052, 2000.
- Landreman, A. P., Shafer, M. M., Hemming, J. C., Hannigan, M. P., and Schauer, J. J.: A macrophage-based method for the assessment of the Reactive Oxygen Species (ROS) activity of atmospheric particulate matter (PM) and application to routine (daily-24 h) aerosol monitoring studies, *Aerosol Sci. Technol.*, 42, 946–957, doi:10.1080/02786820802363819, 2008.
- Li, Q. F., Wyatt, A., and Kamens, R. M.: Oxidant generation and toxicity enhancement of aged-diesel exhaust, *Atmos. Environ.*, 43, 1037–1042, doi:10.1016/j.atmosenv.2008.11.018, 2009.
- Li, R., Ning, Z., Majumdar, R., Cui, J., Takabe, W., Jen, N., Sioutas, C., and Hsiai, T.: Ultrafine particles from diesel vehicle emissions at different driving cycles induce differential vascular pro-inflammatory responses: Implication of chemical components and NF-kappaB signaling, *Particle Fibre Toxicol.*, 7, 6, doi:10.1186/1743-8977-7-6, 2010.
- Liochev, S. I. and Fridovich, I.: The Haber-Weiss cycle – 70 years later: an alternative view, Redox report: communications in free radical research, 7, 55–57, doi:10.1179/135100002125000190, 2002.
- Lundstedt, S., White, P. A., Lemieux, C. L., Lynes, K. D., Lambert, I. B., Öberg, L., Haglund, P., and Tysklind, M.: Sources, fate, and toxic hazards of oxygenated polycyclic aromatic hydrocarbons (PAHs) at PAH-contaminated sites, *AMBIO: A Journal of the Human Environment*, 36, 475–485, doi:10.1579/0044-7447(2007)36[475:sfatho]2.0.co;2, 2007.
- Maynard, D., Coull, B. A., Gryparis, A., and Schwartz, J.: Mortality risk associated with short-term exposure to traffic particles and sulfates, *Environ. Health Perspect.*, 115, 751–755, doi:10.1289/ehp.9537, 2007.
- Metzger, K. B., Tolbert, P. E., Klein, M., Peel, J. L., Flanders, W. D., Todd, K., Mulholland, J. A., Ryan, P. B., and Frumkin, H.: Ambient air pollution and cardiovascular emergency department visits, *Epidemiology*, 15, 46–56, doi:10.1097/01.EDE.0000101748.28283.97, 2004.
- Minguillón, M. C., Cirach, M., Hoek, G., Brunekreef, B., Tsai, M., de Hoogh, K., Jedynska, A., Kooter, I. M., Nieuwenhuijsen, M., and Querol, X.: Spatial variability of trace elements and sources for improved exposure assessment in Barcelona, *Atmos. Environ.*, 89, 268–281, doi:10.1016/j.atmosenv.2014.02.047, 2014.
- Nel, A. E., Diaz-Sanchez, D., and Li, N.: The role of particulate pollutants in pulmonary inflammation and asthma: evidence for the involvement of organic chemicals and oxidative stress, *Current Opin. Pulm. Med.*, 7, 20–26, doi:10.1097/00063198-200101000-00004, 2001.
- Oakes, M., Ingall, E. D., Lai, B., Shafer, M. M., Hays, M. D., Liu, Z. G., Russell, A. G., and Weber, R. J.: Iron solubility related to particle sulfur content in source emission and ambient fine particles, *Environ. Sci. Technol.*, 46, 6637–6644, doi:10.1021/es300701c, 2012.
- Paatero, P. and Tapper, U.: Positive matrix factorization: A non-negative factor model with optimal utilization of error estimates of data values, *Environmetrics*, 5, 111–126, doi:10.1002/env.3170050203, 1994.

- Peel, J. L., Tolbert, P. E., Klein, M., Metzger, K. B., Flanders, W. D., Todd, K., Mulholland, J. A., Ryan, P. B., and Frumkin, H.: Ambient air pollution and respiratory emergency department visits, *Epidemiology*, 16, 164–174, doi:10.1097/01.ede.0000152905.42113.db, 2005.
- Polissar, A. V., Hopke, P. K., Paatero, P., Malm, W. C., and Sisler, J. F.: Atmospheric aerosol over Alaska: 2. Elemental composition and sources, *J. Geophys. Res.-Atmos.*, 103, 19045–19057, doi:10.1029/98JD01212, 1998.
- Pope, C. A., Burnett, R. T., Thun, M. J., Calle, E. E., Krewski, D., Ito, K., and Thurston, G. D.: Lung cancer, cardiopulmonary mortality, and long-term exposure to fine particulate air pollution, *J. Am. Med. Assoc.*, 287, 1132–1141, doi:10.1001/jama.287.9.1132, 2002.
- Pope, C. A., Burnett, R. T., Thurston, G. D., Thun, M. J., Calle, E. E., Krewski, D., and Godleski, J. J.: Cardiovascular mortality and long-term exposure to particulate air pollution: epidemiological evidence of general pathophysiological pathways of disease, *Circulation*, 109, 71–77, doi:10.1161/01.CIR.0000108927.80044.7F, 2004.
- Raizenne, M., Neas, L. M., Damokosh, A. I., Dockery, D. W., Spengler, J. D., Koutrakis, P., Ware, J. H., and Speizer, F. E.: Health effects of acid aerosols on North American children: pulmonary function, *Environ. Health Perspect.*, 104, 506–514, doi:10.2307/3432991, 1996.
- Richard, A., Gianini, M. F. D., Mohr, C., Furger, M., Bukowiecki, N., Minguillón, M. C., Lienemann, P., Flechsig, U., Appel, K., DeCarlo, P. F., Heringa, M. F., Chirico, R., Baltensperger, U., and Prévôt, A. S. H.: Source apportionment of size and time resolved trace elements and organic aerosols from an urban courtyard site in Switzerland, *Atmos. Chem. Phys.*, 11, 8945–8963, doi:10.5194/acp-11-8945-2011, 2011.
- Riediker, M., Devlin, R., Griggs, T., Herbst, M., Bromberg, P., Williams, R., and Cascio, W.: Cardiovascular effects in patrol officers are associated with fine particulate matter from brake wear and engine emissions, *Particle Fibre Toxicol.*, 1, 2, doi:10.1186/1743-8977-1-2, 2004.
- Saffari, A., Daher, N., Shafer, M. M., Schauer, J. J., and Sioutas, C.: Global perspective on the oxidative potential of airborne particulate matter: a synthesis of research findings, *Environ. Sci. Technol.*, 48, 7576–7583, doi:10.1021/es500937x, 2014.
- Sarnat, J. A., Marmur, A., Klein, M., Kim, E., Russell, A. G., Sarnat, S. E., Mulholland, J. A., Hopke, P. K., and Tolbert, P. E.: Fine particle sources and cardiorespiratory morbidity: an application of chemical mass balance and factor analytical source-apportionment methods, *Environ. Health Perspect.*, 116, 459–466, doi:10.1289/ehp.10873, 2008.
- Sauvain, J.-J., Deslarzes, S., and Riediker, M.: Nanoparticle reactivity toward dithiothreitol, *Nanotoxicology*, 2, 121–129, doi:10.1080/17435390802245716, 2008.
- Seagrave, J., McDonald, J. D., Gigliotti, A. P., Nikula, K. J., Seilkop, S. K., Gurevich, M., and Mauderly, J. L.: Mutagenicity and in vivo toxicity of combined particulate and semivolatile organic fractions of gasoline and diesel engine emissions, *Toxicol. Sci.*, 70, 212–226, doi:10.1093/toxsci/70.2.212, 2002.
- Seagrave, J., Gigliotti, A., McDonald, J. D., Seilkop, S. K., Whitney, K. A., Zielinska, B., and Mauderly, J. L.: Composition, toxicity, and mutagenicity of particulate and semivolatile emissions from heavy-duty compressed natural gas-powered vehicles, *Toxicological Sci.*, 87, 232–241, doi:10.1093/toxsci/kfi230, 2005.
- Shakya, K. M. and Peltier, R. E.: Non-sulfate sulfur in fine aerosols across the United States: Insight for organosulfate prevalence, *Atmos. Environ.*, 100, 159–166, doi:10.1016/j.atmosenv.2014.10.058, 2015.
- Shen, H. and Anastasio, C.: Formation of hydroxyl radical from San Joaquin Valley particles extracted in a cell-free surrogate lung fluid, *Atmos. Chem. Phys.*, 11, 9671–9682, doi:10.5194/acp-11-9671-2011, 2011.
- Shi, T., Schins, R. P., Knaapen, A. M., Kuhlbusch, T., Pitz, M., Heinrich, J., and Borm, P. J.: Hydroxyl radical generation by electron paramagnetic resonance as a new method to monitor ambient particulate matter composition, *J. Environ. Monitor.*, 5, 550–556, doi:10.1039/B303928P, 2003.
- Sternbeck, J., Sjödin, Å., and Andréasson, K.: Metal emissions from road traffic and the influence of resuspension – results from two tunnel studies, *Atmos. Environ.*, 36, 4735–4744, doi:10.1016/S1352-2310(02)00561-7, 2002.
- Stohs, S. J. and Bagchi, D.: Oxidative mechanisms in the toxicity of metal ions, *Free Radical Bio. Med.*, 18, 321–336, doi:10.1016/0891-5849(94)00159-H, 1995.
- Strak, M., Janssen, N. A., Godri, K. J., Gosens, I., Mudway, I. S., Cassee, F. R., Lebret, E., Kelly, F. J., Harrison, R. M., Brunekreef, B., Steenhof, M., and Hoek, G.: Respiratory health effects of airborne particulate matter: the role of particle size, composition, and oxidative potential—the RAPTES project, *Environ. Health Perspect.*, 120, 1183–1189, doi:10.1289/ehp.1104389, 2012.
- Sullivan, A. P., Peltier, R. E., Brock, C. A., de Gouw, J. A., Holloway, J. S., Warneke, C., Wollny, A. G., and Weber, R. J.: Airborne measurements of carbonaceous aerosol soluble in water over northeastern United States: Method development and an investigation into water-soluble organic carbon sources, *J. Geophys. Res.-Atmos.*, 111, D23S46, doi:10.1029/2006JD007072, 2006.
- Tolocka, M. P. and Turpin, B.: Contribution of organosulfur compounds to organic aerosol mass, *Environ. Sci. Technol.*, 46, 7978–7983, doi:10.1021/es300651v, 2012.
- Torre, C., Mattutino, G., Vasino, V., and Robino, C.: Brake linings: a source of non-GSR particles containing lead, barium, and antimony, *J. Forensic Sci.*, 47, 494–504, 2002.
- Turn, S. Q., Jenkins, B. M., Chow, J. C., Pritchett, L. C., Campbell, D., Cahill, T., and Whalen, S. A.: Elemental characterization of particulate matter emitted from biomass burning: Wind tunnel derived source profiles for herbaceous and wood fuels, *J. Geophys. Res.-Atmos.*, 102, 3683–3699, doi:10.1029/96jd02979, 1997.
- Valko, M., Morris, H., and Cronin, M. T.: Metals, toxicity and oxidative stress, *Curr. Med. Chem.*, 12, 1161–1208, doi:10.2174/0929867053764635, 2005.
- Verma, V., Shafer, M. M., Schauer, J. J., and Sioutas, C.: Contribution of transition metals in the reactive oxygen species activity of PM emissions from retrofitted heavy-duty vehicles, *Atmos. Environ.*, 44, 5165–5173, doi:10.1016/j.atmosenv.2010.08.052, 2010.
- Verma, V., Rico-Martinez, R., Kotra, N., King, L. E., Liu, J., Snell, T. W., and Weber, R. J.: Contribution of water-soluble and insoluble components and their hydrophobic/hydrophilic sub-fractions to the reactive oxygen species-generating potential of

- fine ambient aerosols, *Environ. Sci. Technol.*, 46, 11384–11392, doi:10.1021/es302484r, 2012.
- Verma, V., Fang, T., Guo, H., King, L., Bates, J. T., Peltier, R. E., Edgerton, E., Russell, A. G., and Weber, R. J.: Reactive oxygen species associated with water-soluble PM<sub>2.5</sub> in the southeastern United States: spatiotemporal trends and source apportionment, *Atmos. Chem. Phys.*, 14, 12915–12930, doi:10.5194/acp-14-12915-2014, 2014.
- Verma, V., Fang, T., Xu, L., Peltier, R. E., Russell, A. G., Ng, N. L., and Weber, R. J.: Organic aerosols associated with the generation of Reactive Oxygen Species (ROS) by water-soluble PM<sub>2.5</sub>, *Environ. Sci. Technol.*, 49, 4646–4656, doi:10.1021/es505577w, 2015.
- Wilson, J. G., Kingham, S., Pearce, J., and Sturman, A. P.: A review of intraurban variations in particulate air pollution: Implications for epidemiological research, *Atmos. Environ.*, 39, 6444–6462, doi:10.1016/j.atmosenv.2005.07.030, 2005.
- Zhang, X., Hecobian, A., Zheng, M., Frank, N. H., and Weber, R. J.: Biomass burning impact on PM<sub>2.5</sub> over the southeastern US during 2007: integrating chemically speciated FRM filter measurements, MODIS fire counts and PMF analysis, *Atmos. Chem. Phys.*, 10, 6839–6853, doi:10.5194/acp-10-6839-2010, 2010.
- Zhang, Y., Schauer, J. J., Shafer, M. M., Hannigan, M. P., and Dutton, S. J.: Source apportionment of in vitro Reactive Oxygen Species bioassay activity from atmospheric particulate matter, *Environ. Sci. Technol.*, 42, 7502–7509, doi:10.1021/es800126y, 2008.